The Canadian Mineralogist
Vol. 33, pp. 609-626 (1995)

THE INFRARED SPECTROSCOPY OF VESUVIANITE IN THE OH REGION

LEE A. GROAT
Department of Geological Sciences, University of British Columbia, Vancouver, British Columbia V6T 1Z4

FRANK C. HAWTHORNE
Department of Geological Sciences, University of Manitoba, Winnipeg, Manitoba R3T 2N2

GEORGE R. ROSSMAN
Division of Geological and Planetary Sciences, California Institute of Technology, Pasadena, California 91125, U.S.A.

T. SCOTT ERCIT
Canadian Museum of Nature, Mineral Sciences Section, Ottawa, Ontario K1P 6P4

Abstract

Many important substitutions in vesuvianite involve variable H, and those that do not still perturb the local environment of the OH^- anions. Consequently, infrared spectroscopy of the OH fundamental and overtone regions is an important probe of local order. We have examined a series of vesuvianite crystals carefully characterized (by electron-microprobe analysis, wet-chemical analysis and crystal-structure refinement) by polarized single-crystal infrared spectroscopy. The crystals span the complete range of chemical variation reported in vesuvianite, and the spectra show tremendous variability. There are 13 recognizable bands (*A–M*) that can be divided into three types: (1) eight bands due to absorptions at the *OH* site; these result from different local cation and anion configurations at nearest-neighbor and next-nearest-neighbor sites; (2) four bands due to absorption at *O*(10); these result from different local cation and anion configurations at nearest-neighbor and next-nearest-neighbor sites, and (3) a low-energy electronic absorption band. Boron is incorporated into the vesuvianite structure primarily *via* the substitution $B + Mg \rightleftharpoons 2H + Al$. In boron-rich vesuvianite, the four bands *J–M* are not present, indicating that H has been completely replaced by B in the vicinity of the *O*(10) site. Although lacking the fine detail of the principal-stretching region, the overtone spectra are equally characteristic of this B↔H substitution. The spectra in the principal OH-stretching region extend over a very wide spectral range (3700–3000 cm^{-1}), and show two features that are of *general* importance in the quantitative interpretation of such spectra: (1) the band width increases significantly with decreasing band-frequency (from ~20 cm^{-1} at 3670 cm^{-1} to ~120 cm^{-1} at 3060 cm^{-1}), and (2) the band intensity is (nonlinearly) correlated with band frequency (in addition to H content). These two features are of significance in quantitatively fitting spectra by numerical techniques, and in relating band intensities to compositional features.

Keywords: vesuvianite, infrared spectra, electron-microprobe analysis, crystal structure, hydroxyl.

Sommaire

Plusieurs schémas de substitution impliquent l'hydrogène dans la vésuvianite, et ceux qui ne l'impliquent pas directement affectent quand même le voisinage des anions OH. Par conséquent, la spectroscopie des vibrations fondamentales et des harmoniques dans l'infrarouge peut fournir une information précieuse à propos du degré d'ordre local. Nous avons examiné par spectroscopie infrarouge polarisée sur cristal unique une série d'échantillons bien caractérisés chimiquement par analyse à la microsonde électronique, par voie humide, et par affinement de la structure cristalline. Les cristaux représentent la gamme complète de variations chimiques décrites dans la vésuvianite, et les spectres font preuve d'une variabilité imposante. Le spectre comprend treize bandes distinctes (*A–M*) qui sont divisibles en trois catégories: (1) huit bandes attribuées aux absorptions au site *OH*, qui découlent des différents agencements locaux des cations et des anions impliquant les proches voisins et les deuxièmes plus proches voisins; (2) quatre bandes dues à l'absorption dans le site *O*(10), qui découlent des différents agencements locaux des cations et des anions impliquant les proches voisins et les deuxièmes plus proches voisins, et (3) une bande attribuable à une absorption électronique de faible énergie. Le bore est incorporé dans la structure surtout selon la substitution $B + Mg \rightleftharpoons 2H + Al$. Dans la vésuvianite borifère, les quatre bandes *J–M* ne sont pas présentes, ce qui indique que le B remplace complètement le H dans le voisinage du site *O*(10). Malgré l'absence de résolution fine dans la région de l'étirement principal des bandes OH, les spectres des harmoniques sont également caractéristiques de cette substitution B↔H. Cette région des spectres s'étend sur un grand intervalle (3700–3000 cm^{-1}), et montre deux aspects d'importance générale dans l'interprétation quantitative de tels spectres: (1) la largeur des bandes augmente de façon importante à mesure que diminue la fréquence de la bande, d'environ 20 cm^{-1} à 3670 cm^{-1} jusqu'à environ 120 cm^{-1} à 3060 cm^{-1}; (2) l'intensité des bandes montre une corrélation non linéaire avec la fréquence de la bande, et en plus avec la teneur en H. Ces deux généralisations ont une importance capitale dans l'interprétation quantitative des spectres et dans l'attribution des intensités des bandes aux traits compositionnels.

(Traduit par la Rédaction)

Mots-clés: vésuvianite, spectre infrarouge, analyse à la microsonde électronique, structure cristalline, hydroxyle.

INTRODUCTION

Although the general arrangement of the vesuvianite structure has been known since the work of Warren & Modell (1931), there are still details of its crystal chemistry that remain obscure. Groat *et al.* (1992a) showed that the general formula of vesuvianite can be written $X_{19}\,Y_{13}\,T_5\,Z_{18}\,O_{68}\,W_{10}$, where X = Ca, Na, *REE*, Pb^{2+}, Sb^{3+}, Y = Al, Mg, Fe^{2+}, Fe^{3+}, Mn, Ti, Cr, Cu, Zn, T = □, B, Z = Si, and W = OH, F, O^{2-}. A particularly important aspect of this work was the recognition (or rather the re-emphasis) of the importance of boron in vesuvianite from some localities. Groat *et al.* (1992a) proposed that B is incorporated into the vesuvianite structure *via* a substitution that is particularly difficult to recognize solely on the basis of electron-microprobe data: B + Mg ⇌ 2H + Al. This situation is further complicated by the fact that B also can be incorporated by a mechanism that involves the substitution of *REE* for Ca at the *X* positions in the structure.

Groat *et al.* (1994a) showed that B occurs at two distinct sites in the structure, sites that are unoccupied in B-free vesuvianite. The local details around these sites are somewhat obscured by extensive positional disorder. Nevertheless, it is apparent that B locally replaces H in the structure. Many important substitutions in vesuvianite involve variable amounts of hydrogen incorporated *via* $(OH)^- \rightleftharpoons O^{2-}$ exchange. Because of this, infrared spectroscopy in the (OH)-stretching region should be a useful probe of local stereochemical variations in the vicinity of the *O*(10) and *OH* sites in the vesuvianite structure. Consequently, this study was initiated in parallel with the concurrent work on the chemistry and structure of vesuvianite (Groat *et al.* 1992a, b, 1993, 1994a, b).

EXPERIMENTAL

The samples used in this work are listed in Table 1; the letter coding corresponds to that of Groat *et al.* (1992a). Oriented sections of single crystals were cut using, where possible, the external morphology as a guide, and the orientations of the resulting sections were checked by optical interference figures. For samples with no external morphology, crystals were oriented by X-ray precession photography, sunk into a block of 5-minute® epoxy and then sawn into slices of appropriate orientation and thickness. Sections 2.0–0.5 mm thick were ground and doubly polished for optical and electron-microprobe measurements. The sections were then removed from the glass slides, remounted with Crystalbond® adhesive, handground to a thickness in the range 10–90 μm, depending on the H content, and then polished. Most sections were then removed from their glass slide with acetone. Some very delicate samples were left mounted; for these, it was necessary to subtract a background due to the glass slide and also to remove the spectral contribution of the adhesive.

TABLE 1. VESUVIANITE SAMPLES USED FOR INFRARED SPECTROSCOPIC WORK

#	Locality	Qualitative chemical description
V4	Turnback Lake, N.W.T.	F-rich, low-Al, high-Fe^{3+}
V5	Long Lake Mine, Olden Twp., Ont.	F-rich, high-Al
V6	York River, Dungannon Twp., Ont.	F-rich, low-Fe
V11	Jeffrey Mine, Richmond Co., Que.	F-free, high-Al, low-Fe, Ti-free
V13	Jeffrey Mine, Richmond Co., Que.	F-free, high-Al
V23	Laurel, Que.	F-free, high-Fe^{3+}/Fe^{2+}
V28	Templeton Twp., Ottawa Co., Que.	Int-F, Ti-rich
V30	Templeton Twp., Ottawa Co., Que.	Int-F, B-rich, low-OH
V31	Wakefield twp., Ottawa Co., Que.	Int-F, Ti-rich
V33	Mame Claim, Y.T.	F-rich
V36	Ariccia, Rome, Italy	Int-F, Int-B, high-REE
V45	Laguna del Jaco, Chihuahua, Mexico	Int-F, Int-B
V49	Hindubagh, Baluchistan, Pakistan	F-rich Ti-free, high-Al, low-Fe
V75	Wilui River, Yakutskaya, Russia	F-free, B-rich, low-OH
ALA	Val d'Ala, Piemonte, Italy	
GEM	Tanzania	

Chemical analysis

Chemical analyses were done with a JEOL 733 electron microprobe fitted with one energy-dispersion spectrometer and four automated wavelength-dispersion spectrometers. A detailed description of the analytical procedures was given by Groat *et al.* (1992a). For some samples, H_2O and Fe^{2+}/Fe^{3+} ratios were determined as described by Groat *et al.* (1992a). Because of the amount of sample required for these measurements, bulk samples had to be used for all crystals, including those showing sector zoning; thus we have no direct information on the variation of these components in single crystals.

Infrared spectroscopy

Infrared spectra were measured on a Nicolet 60SX FTIR spectrometer fitted with a rotatable glan-Foucault $LiIO_3$ crystal polarizer; apertures (50–200 μm in diameter) were used to limit the area of the sample exposed to the beam. Crystal fragments were examined with a polarizing-light microscope, and points were selected for measurement on the basis of crystal quality (absence of alteration, cracks and inclusions within the field of the aperture); the crystal was then oriented on a polarizing microscope prior to insertion into the spectrometer.

RESULTS

Chemical analysis

Compositional data for the crystals of Table 1 are given in Table 2. The unit formulae were calculated

TABLE 2. AVERAGE CHEMICAL COMPOSITIONS (wt.%) AND UNIT FORMULAE* OF VESUVIANITE CRYSTALS USED FOR INFRARED SPECTROSCOPY

	V4	V5	V6	V11	V13	V23	V28	V30	V31	V33	V38	V45	V49	V75
SiO_2	36.22	36.56	35.92	36.85	36.53	37.56	36.80	34.83	36.76	37.54	34.99	36.39	37.01	36.00
Al_2O_3	16.00	16.90	15.91	18.79	17.90	17.96	16.15	11.31	16.47	17.33	12.00	15.21	18.81	11.72
TiO_2	1.43	0.96	1.14	0.00	0.60	0.00	2.77	0.94	2.73	0.67	1.36	0.73	0.00	0.34
MgO	1.57	1.77	2.72	1.80	1.71	2.56	1.76	4.74	1.56	1.76	4.69	3.93	1.96	6.75
MnO	0.35	0.40	0.78	0.89	0.06	0.18	0.00	0.25	0.00	0.74	0.27	0.19	0.78	0.08
FeO	2.38	2.86	1.91	1.14	1.36	0.29	2.61	5.32	2.70	3.16	5.07	3.64	0.60	1.56
Fe_2O_3**	3.06	1.18	–	–	1.83	1.11	–	–	–	0.37	–	–	–	2.96
CaO	34.78	35.33	34.27	36.17	35.56	36.85	35.97	33.11	35.58	35.43	34.63	35.90	36.29	35.60
Na_2O	0.17	0.03	0.03	0.07	0.00	0.00	0.13	0.01	0.23	0.10	0.00	0.00	0.07	0.00
Ln_2O_3++	0.10	0.00	0.97	0.00	0.00	0.00	0.00	3.16	0.00	0.00	1.58	0.00	0.00	0.10
B_2O_3	0.00	0.00	0.00	0.00	0.00	0.00	0.00	2.90	0.00	0.00	1.77	1.47	–	2.83
F	1.97	2.26	2.44	0.00	0.00	0.00	1.30	0.75	1.55	3.10	0.73	0.32	2.65	0.28
Cl	0.19	0.04	0.81	0.00	0.01	0.00	0.21	0.00	0.15	0.00	0.00	0.00	0.00	0.00
H_2O†	1.56	1.70	–	2.77	–	–	–	–	–	1.63	–	–	–	0.61
H_2O‡	1.53	1.49	1.32	2.82	2.55	2.78	1.79	0.50	1.67	1.31	1.89	1.49	1.59	0.87
	99.75	99.99	98.22	98.48	98.11	99.29	99.50	97.83	99.40	101.83	98.98	99.13	100.31	98.83
O=F,Cl	0.91	1.01	1.21	0.00	0.00	0.00	0.60	0.32	0.68	1.31	0.31	0.14	1.12	0.11
TOTAL	98.84	98.98	97.01	98.48	98.11	99.29	98.90	97.51	98.72	100.52	98.67	98.99	99.19	98.72

TABLE 2. continued.

	V4	V5	V6	V11	V13	V23	V28	V30	V31	V33	V38	V45	V49	V75
Si	17.98	18.03	18.15	18.02	18.03	18.19	18.13	18.06	18.13	18.26	17.64	17.97	18.02	17.92
Al	9.36	9.83	9.47	10.83	10.41	10.25	9.32	6.91	9.57	9.94	7.13	8.66	10.79	6.88
Ti^{4+}	0.53	0.36	0.43	0.00	0.22	0.00	1.03	0.37	1.01	0.25	0.52	0.54	0.00	0.13
Mg	1.16	1.30	2.05	1.31	1.26	1.85	1.29	3.66	1.15	1.28	3.53	2.89	1.42	5.01
Mn^{2+}	0.15	0.17	0.33	0.37	0.03	0.07	0.00	0.11	0.00	0.31	0.12	0.08	0.32	0.03
Fe^{2+}	0.99	1.18	0.81	0.47	0.56	0.12	1.08	2.31	1.11	1.29	2.14	1.50	0.24	0.65
Fe^{3+}	1.14	0.44	–	–	0.68	0.40	–	–	0.00	0.14	–	–	–	0.55
Ca	18.50	18.67	18.55	18.95	18.81	19.12	18.98	18.39	18.80	18.46	18.71	19.00	18.93	18.99
Na	0.16	0.03	0.03	0.07	0.00	0.00	0.12	0.01	0.22	0.09	0.00	0.00	0.07	0.00
Ln^{3+}	0.02	0.00	0.18	0.00	0.00	0.00	0.00	0.60	0.00	0.00	0.30	0.00	0.00	0.01
B	0.00	0.00	0.00	0.00	0.00	0.00	0.00	2.60	0.00	0.00	1.54	1.25	–	2.43
F	3.09	3.53	3.90	0.00	0.00	0.00	2.03	1.23	2.42	4.77	1.16	1.00	4.08	0.44
Cl	0.16	0.03	0.69	0.00	0.01	0.00	0.18	0.00	0.13	0.00	0.00	0.00	0.00	0.00
OH	5.17	5.59	4.44	9.21	8.39	8.97	5.89	1.74	5.51	5.29	6.34	4.91	5.15	2.03
ΣX	18.68	18.70	18.76	19.01	18.81	19.12	19.11	19.00	19.02	18.55	19.00	19.00	19.00	19.00
ΣY	13.32	13.27	13.10	12.97	13.16	12.69	12.77	13.36	12.85	13.21	13.07	13.87	12.98	13.25
ΣZ	17.98	18.03	18.15	18.02	18.03	18.19	18.13	18.06	18.13	18.26	18.00	17.97	18.02	17.92

*Analyses of boron-bearing vesuvianite are normalized on 19 *X*-cations; those of boron-free vesuvianite on 50 total cations.
** Fe_2O_3 values taken from Groat *et al.* (1992a). + – = not determined. ++ Ln_2O_3 = REE content. †Measured. ‡Calculated.
Additional components (wt.%): V4, Ce_2O_3 0.10; V6, La_2O_3 0.29, Ce_2O_3 0.68; V30, La_2O_3 1.17, Ce_2O_3 1.55, Pr_2O_3 0.16, Nd_2O_3 0.19, Gd_2O_3 0.09; V33, BeO 0.15; V38, La_2O_3 0.84, Ce_2O_3 0.74; V49, CuO 0.55; V75, BeO 0.03, La_2O_3 0.09, Ce_2O_3 0.22.

according to the recommendations of Groat *et al.* (1992a).

Infrared spectroscopy

The polarized spectra in the fundamental hydroxyl-stretching region (3000–3800 cm^{-1}) and the first overtone hydroxyl-stretching region (6500–7500 cm^{-1}) are shown in Figures 1 and 2. Band positions are

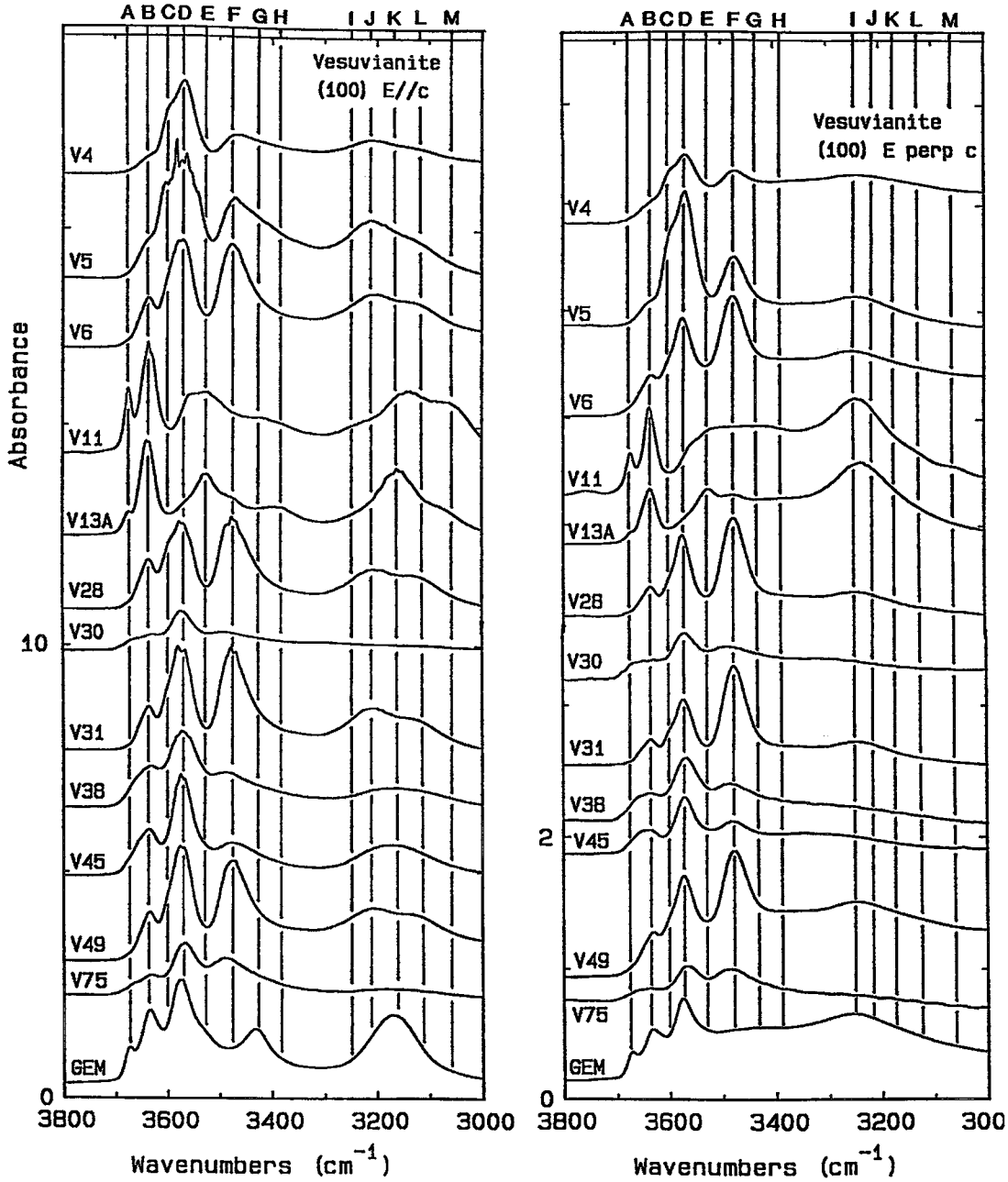

FIG. 1. The polarized absorption-spectra of vesuvianite crystals in the principal hydroxyl-stretching region: (a) E $\parallel$ *c*; (b) E $\perp$ *c*; band positions are shown by the vertical lines, with the band label at the top of the figure.

marked by vertical lines, and band labels are given on each figure. Band positions and polarizations are given in Tables 3 and 4; for the polarization behavior, relative intensities were measured from the absorbance spectra with a mm scale after interpolation of a background by eye. We had originally intended to measure the inten-

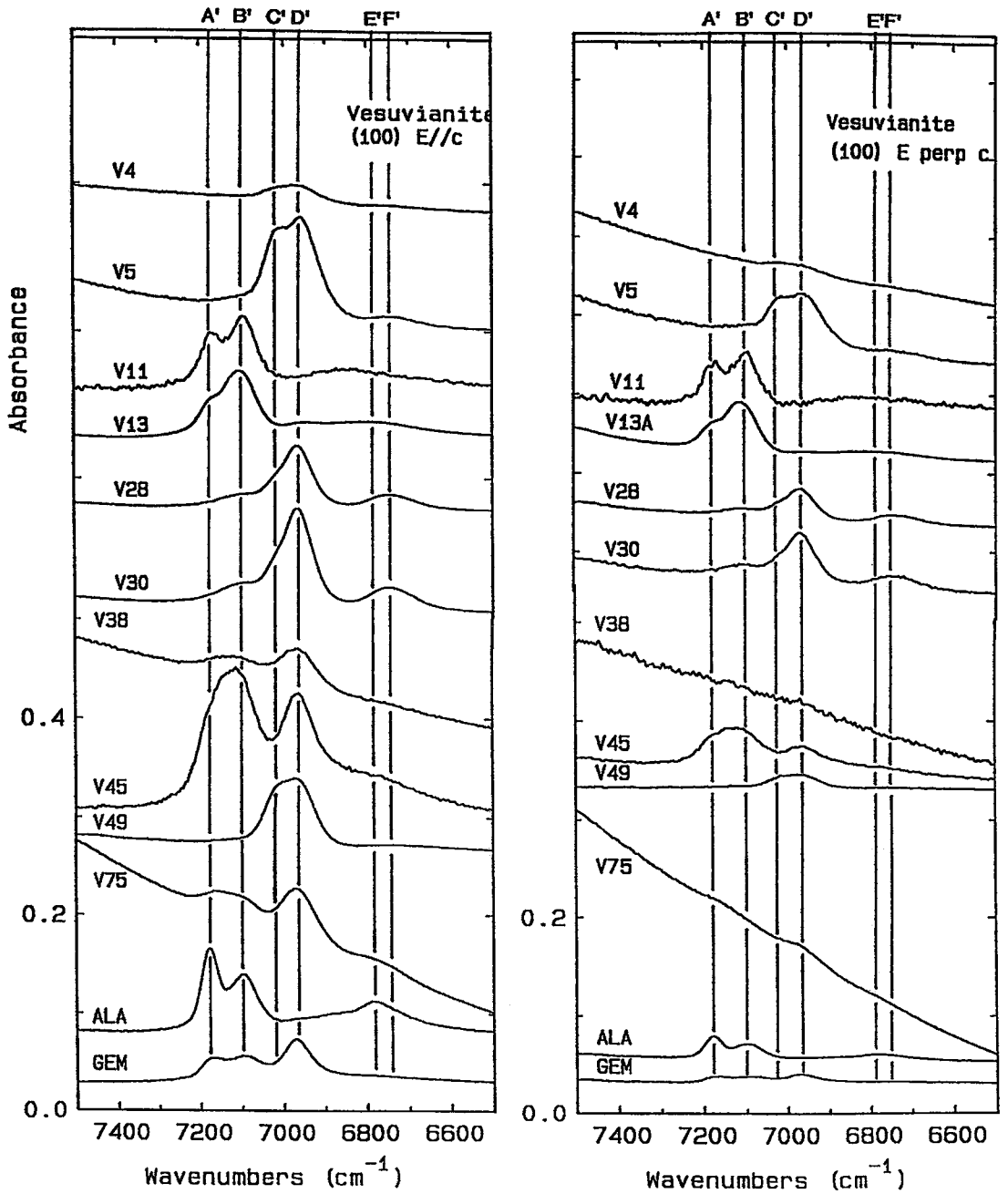

FIG. 2. The polarized absorption-spectra of vesuvianite crystals in the hydroxyl-stretching overtone region: (a) E $\parallel$ c; (b) E $\perp$ c; legend as for Figure 1.

sities of the absorption bands for all spectra using non-linear least-squares refinement. This turned out to be completely intractable. There are up to 14 bands in each spectrum, and the band overlap is extreme. The band shape is very non-Gaussian. Much experimentation with band shape led to the conclusion that a

TABLE 3. BAND POSITIONS AND POLARIZATIONS* IN THE PRINCIPAL OH-STRETCHING REGION OF VESUVIANITE

Band	Position (cm^{-1})	E∥c	E⊥c	Site
A	3670	84	16	*OH*
B	3635	82	18	*OH*
C	3596	*s*	*w*	*OH*
D	3567	85	15	*OH*
E	3524	~80	~20	*OH*
F	3487	75	25	*OH*
G	3430	*ss*	*vw*	*OH*
H	3383	*s*	*w*	*OH*
I	3240	–	100	–
J	3210	100	–	*O*(10)
K	3156	100	–	*O*(10)
L	3120	100	–	*O*(10)
M	3054	100	–	*O*(10)

* band intensities are normalized to 100 for each spectrum; *ss* = very strong, *s* = strong, *w* = weak, *vw* = very weak.

TABLE 4. BAND POSITIONS AND POLARIZATIONS IN THE FIRST OH-OVERTONE REGION OF VESUVIANITE

Band*	Position (cm^{-1})	+E∥c	+E⊥c	Fundamental	$**\nu^O/2\nu^F$
A'	7176	8	2	*A*	0.978
B'	7098	7	3	*B*	0.976
C'	7015	8	2	*C*	0.975
D'	6968	8	2	*D*	0.977
E'	6780	8	2	*E*	0.962
F'	6746	8	2	*F*	0.967
K'	5930	*w*	–	*K*	0.939

* the primed letters are used to distinguish overtone bands from fundamental bands;
** ν^O and ν^F are the frequencies of the overtone and fundamental bands, respectively;
+ band intensities are normalized to 10 for each spectrum, except for *K'*, in which the band is not visible in the E⊥c spectrum.

Pearson-VII function (Howard & Preston 1989) best fitted the data, but the broad tails that occur with this shape produced major uncertainties in the fitting process; slight changes in the shape function produced major changes in the final fit. After much effort, this approach was abandoned.

In some cases, it was not possible to measure both overtone and fundamental spectra owing to sample constraints, primarily the presence of numerous cracks, inclusions, and alteration in some of the samples. There is no evidence for H_2O groups in crystalline vesuvianite, although spectral features characteristic of H_2O were observed in radiation-damaged samples (Eby *et al.* 1993).

Structural Considerations

Although most (if not all) vesuvianite crystals show evidence of departure from tetragonal symmetry, we will refer to the structure in terms of a tetragonal model. Although high-2V crystals do show slight variations in intensity of the principal OH-stretching bands with orientation in (001) sections, this is a very minor effect compared with the spectral differences accompanying compositional differences.

The hydroxyl anion can occupy two sites in the vesuvianite structure, the *OH* site and the *O*(10) site; in order to distinguish between the hydroxyl *anion* and the *OH site* (which may be occupied by hydroxyl or fluorine), we write the former as $(OH)^-$. Both ball-and-stick and polyhedral representations of the *OH* environment are shown in Figure 3. Each *OH* site is coordinated by cations at the *Y*(2), *Y*(3) and *X*(3) sites, and the O–H bond makes an angle of ~30° with the *c* axis. Bond-valence arguments (*e.g.*, Yoshiasa & Matsumoto 1986) show that the *OH* oxygen acts as a strong hydrogen-bond donor, the acceptor anion being *O*(7). The cations coordinating *O*(7) [*Z*(2) and *X*(3)] contribute only ~1.7 v.u. to the anion, and the contribution of ~0.3 v.u. from the *OH*...*O*(7) hydrogen bond is needed for satisfaction of the bond-valence requirement at the *O*(7) anion.

The *O*(10) environment is illustrated in Figure 4. The *O*(10) site lies on the 4-fold axis down the channel through the structure. It is coordinated by one *Y*(1) and four *X*(3) cations in a square pyramidal arrangement. In boron-free vesuvianite, the *O*(10) site is fully occupied; in boron-bearing vesuvianite, *O*(10) is only partially occupied. There have been various proposals as to the identity of the anion occupying the *O*(10) site. The only direct evidence on this point is the neutron structure-refinement of Lager *et al.* (1989), who located a hydrogen (*H*) position asymmetrically placed between two *O*(10) atoms separated by ~2.8 Å along the 4-fold axis parallel to [001]. This *H* site is partly occupied (occupancy = 0.85); the H was assumed to be locally disordered, directly bonded either to the upper *O*(10) oxygen or to the lower *O*(10) oxygen. The details of the geometry around the *O*(10) site in boron-bearing vesuvianite were reported on by Groat *et al.* (1994a). In addition, Groat *et al.* (1992a) have shown that the amount of H is very variable, although the local stereochemical details of this variation are as yet unknown.

Polarization behavior

There are two distinct H positions in the vesuvianite structure, *H*(1) associated with the *OH* site, and *H*(2) associated with the *O*(10) site. For a completely ordered structure, one would expect two bands in the fundamental region, each corresponding to one of the O–H bonds. In a disordered structure, these bands

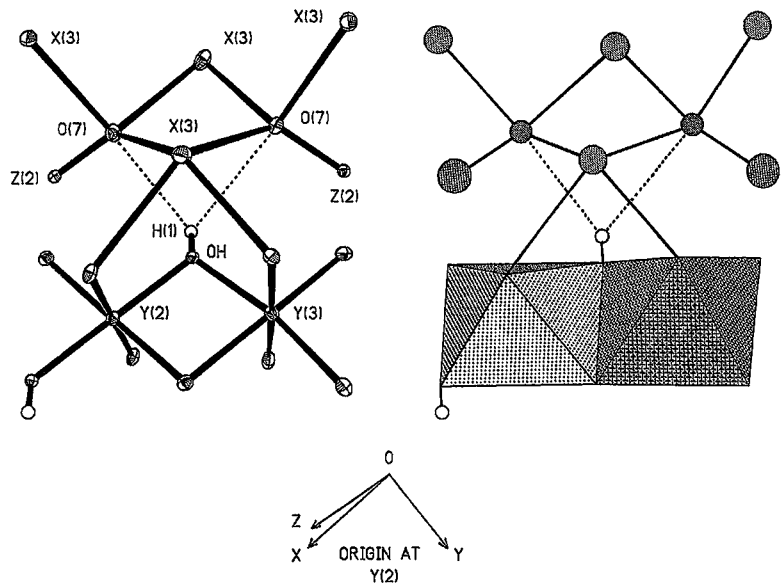

FIG. 3. The *OH* environment in boron-free vesuvianite in both ball-and-stick and polyhedral representations.

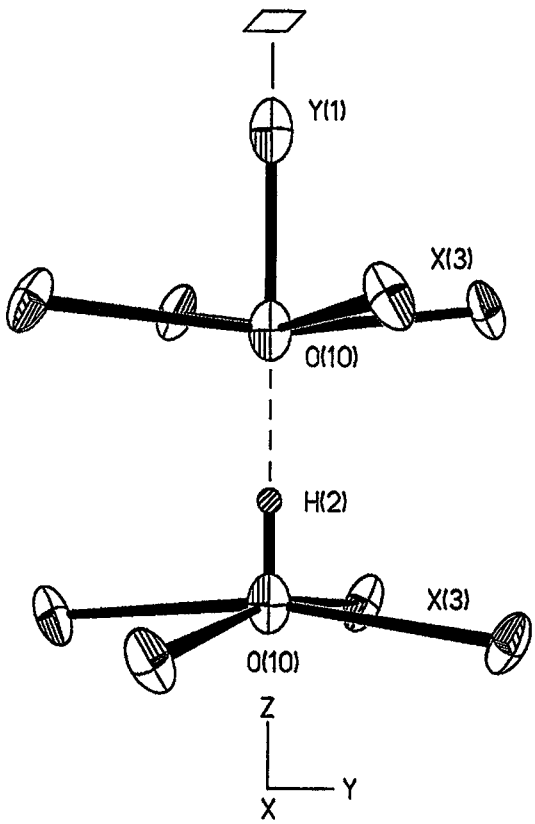

FIG. 4. The *O*(10) environment in boron-free vesuvianite viewed along [100].

can split owing to variations in local environment. According to the long-range structural information available, the polarization behavior of the bands from each of the two H environments should be significantly different. *H*(2) lies on a 4-fold axis, and the O–H bond is along this axis, exactly parallel to the *c* axis; in addition, *H*(2) hydrogen-bonds to the neighboring *O*(10) anion, also on the same 4-fold axis. Thus the fundamental absorption in the infrared will be completely polarized, with maximum intensity E ∥ *c* (electric vector parallel to the *c* axis); it will have zero intensity where E ⊥ *c*. Conversely, the *H*(1) position is so arranged that the *OH*–*H*(1) bond makes an angle of ~30° with the *c* axis. Thus the infrared fundamental band resulting from this bond will be partly polarized, with E ∥ *c* stronger than E ⊥ *c*. Consequently, we can differentiate bands due to *O*(10)–*H*(2) and *OH*–*H*(1) by their different polarization-behavior. Preliminary assignment of the bands in the fundamental hydroxyl-stretching region according to this criterion is shown in Table 3.

Local configurations around OH

It is well known that local disorder at cation positions coordinated by the donor anion of a hydrogen-bonded configuration can produce several bands in the fundamental hydroxyl-stretching region, each corresponding to a different local configuration (Rossman 1988, Hawthorne 1981). A sketch of the relevant local geometry for the *OH* anion is shown in Figure 5. In the linear trimer of edge-sharing octahedra, *Y*(2) is the central octahedron, the two flanking octahedra are

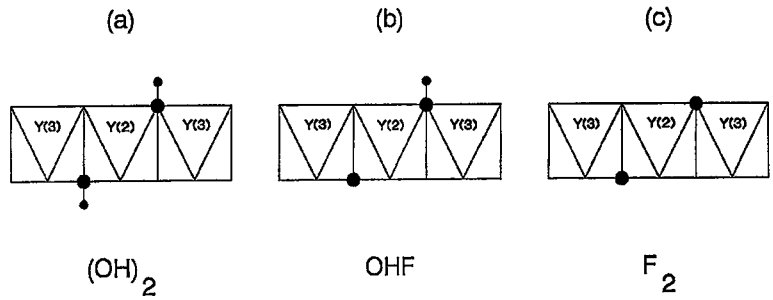

FIG. 5. Idealized sketch of the *OH* position and neighboring polyhedra: (a) the linear *Y*(2)=*Y*(3)=*Y*(2) edge-sharing trimer with hydroxyl at both *OH* positions; (b) *Y*(2)=*Y*(3)=*Y*(2) trimer with one hydroxyl and one fluorine; (c) *Y*(2)=*Y*(3)=*Y*(2) trimer with two fluorine atoms at the *OH* positions.

Y(3), and the corresponding sites can potentially be occupied by Al, Fe (Fe^{3+} and Fe^{2+}), Mg and Ti. There are two *OH* sites in this trimer, arranged in a *trans* configuration relative to the *Y*(2) octahedron and occurring as part of the edge shared between the *Y*(2) and *Y*(3) octahedra. It is clear that variation in occupancy of the *Y*(2) and *Y*(3) sites have the potential to produce distinct bands in the infrared region. Each *OH* site is coordinated to one *Y*(2) and one *Y*(3) cation; it is also adjacent to an *X*(3) cation; however, the *X*(3) site shows insufficient variation in occupancy to produce significant multiple bands. Consequently, the number of bands will be equal to the number of local configurations possible at *Y*(2) and *Y*(3) within the constraints of the known bulk-chemistry and cation-ordering patterns. Not all of these bands may be resolved (owing to accidental band overlap or insufficient intensity of the bands above background).

Local arrangements of cations: The results of crystal-structure refinement (Coda *et al.* 1970, Rucklidge *et al.* 1975, Giuseppetti & Mazzi 1983, Valley *et al.* 1985, Yoshiasa & Matsumoto 1986, Fitzgerald *et al.* 1986a, b, 1987, Groat *et al.* 1992b, 1994b) show that the *Y*(2) site is virtually entirely occupied by Al. Hence, with regard to local configurations about the *OH* site, the *Y*(2) site is fixed (=Al), and any variation occurs at the *Y*(3) site. According to the general chemistry of vesuvianite (Groat *et al.* 1992a), the *Y*(3) site can potentially be occupied by the following *Y*-group cations: Mg, Fe^{2+}, Al, Fe^{3+}, Ti^{4+}. However, crystal-structure refinements of low-Fe Ti-bearing vesuvianite crystals (work in progress) show Ti to be ordered at the *Y*(1) site. Thus Ti^{4+} is not a significant occupant of the *Y*(3) site, which thus can be occupied by Mg, Fe^{2+}, Al and Fe^{3+}; hence there are four possible local cation-configurations about the *OH* site in vesuvianite (Table 5).

Local arrangements of anions: Each *Y*(2) [=Al] cation is adjacent to two *OH* sites in a *trans* configuration (Fig. 5a). Fluorine may be incorporated at the *OH* site in two different ways: F^- may replace $(OH)^-$ at one of the two *OH* sites in the trimer to produce the $(OH)^-$–F^- local arrangement shown in Figure 5b; alternatively, F^- may replace $(OH)^-$ at both *OH* sites to produce the F^-–F^- local arrangement shown in Figure 5c. Replacement of one $(OH)^-$ by one F^- (Fig. 5b) will eliminate one hydroxyl band, and can potentially cause an inductive shift in the band from the remaining $(OH)^-$ *trans* to the substituted F^- anion. Replacement of both $(OH)^-$ anions by F^- (Fig. 5c) will eliminate two hydroxyl bands and will give rise to no new hydroxyl bands from this specific trimer. Hence these two local schemes of order produce very different results in the infrared spectra.

Comparison of spectra from crystals of fluorine-free and fluorine-bearing vesuvianite will give an idea of the local arrangements involved. Inspection of Table 2 shows that V11 and V49 have very similar populations of cations but very different F contents [<0.3 atoms per

TABLE 5. POSSIBLE LOCAL CONFIGURATIONS ABOUT THE *OH* POSITION IN THE VESUVIANITE STRUCTURE

Configuration	*Y(3)–Y(2)–OH/F/O	
	Boron-free	Boron-bearing
1	Mg–Al–OH	Mg–Al–OH
2	Fe^{2+}–Al–OH	Fe^{2+}–Al–OH
3	Al–Al–OH	Al–Al–OH
4	Fe^{3+}–Al–OH	Fe^{3+}–Al–OH
5	Mg–Al–F	Mg–Al–O–B
6	Fe^{2+}–Al–F	Fe^{2+}–Al–O–B
7	Al–Al–F	Al–Al–O–B
8	Fe^{3+}–Al–F	Fe^{3+}–Al–O–B

* Y(3) = (Mg,Fe^{2+},Al,Fe^{3+}); Y(2) = Al

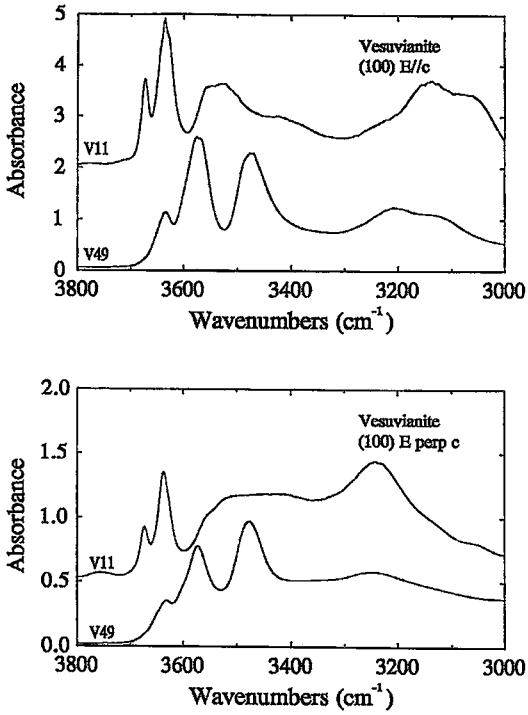

FIG. 6. Comparison of the polarized absorption-spectra of V11 and V49 in the principal hydroxyl-stretching region. V11 and V49 have the same proportions of cations, and differ only in their fluorine content; V11 is very low in fluorine (< 0.6 F apfu), whereas V49 is fluorine-rich (4.1 F apfu).

formula unit (apfu) *versus* 4.1 apfu]. Figure 6 compares the polarized absorption-spectra of these samples in the principal hydroxyl-stretching region. The spectra are strikingly different in both polarizations, indicating that the substitution of F^- for $(OH)^-$ is both suppressing some bands and giving rise to new bands; in particular, band *A* is lost, and band *B* is weakened, whereas other bands, such as *F* and *D*, are new or occur with greatly increased intensity. Hence the $(OH)^-$–F^- arrangement (Fig. 5b) is of major importance in deciphering the local pattern of order around the *OH* site in vesuvianite. There are an *additional* four possible local configurations due to F^- at the next-nearest-neighbor position (Table 5), giving a total of eight bands from the *OH* position. The F^-–F^- configuration produces no new bands, and thus is not directly "visible" in the hydroxyl-stretching spectra. However, the very large effect produced by the incorporation of ~4 F apfu (Fig. 6) into the structure, greatly reducing some bands and producing new dominant bands, indicates that $(OH)^-$–F^- configurations must dominate over F^-–F^- configurations.

Local configurations around O(10)

A sketch of the relevant local geometry for the *O*(10) anion is shown in Figure 4. The *O*(10) anion is coordinated by four *X*(3) cations and one *Y*(1) cation. In most crystals, *X*(3) is completely dominated by Ca, and the only variable occupancy of cations around *O*(10) involves the *Y*(1) site, which may be occupied by Fe^{2+}, Mg, Ti and possibly minor Al and Fe^{3+} (?) (plus Cu^{2+}, Zn and possibly Mn^{3+} in exotic varieties). Most structure refinements have shown transition metals (generally Fe^{2+} and Ti) to dominate at the *Y*(1) site, but other cations (*e.g.*, Mg, Al) have been detected, and hence multiple bands may result.

The *O*(10) anion may also be occupied by F^- (Groat *et al.* 1992b), which alters the strength of the hydrogen bond from the neighboring *O*(10) hydroxyl anion, also potentially producing new band(s) in the hydroxyl-stretching region; as shown in Figure 6, V11 and V49 show significantly different behavior in the low-energy region (3000–3300 cm^{-1}), suggesting that this is the case.

GENERAL FEATURES OF THE SPECTRA

Inspection of Figure 3 shows the extreme variability of the polarized infrared spectra of vesuvianite. Bands *A–H* and *J–M* have been assigned to local *OH* and *O*(10) configurations, respectively, but the detailed assignment of individual bands remains to be done. There are two additional features of the spectra that are rather enigmatic. Firstly, the *I* band, which is prominent in the E ⊥ *c* spectra of V11, V13A and GEM, is incompatible with the orientation of the $(OH)^-$ groups at the *OH* and *O*(10) positions. Secondly, many of the spectra also seem superimposed on a very low-amplitude absorption that extends down to

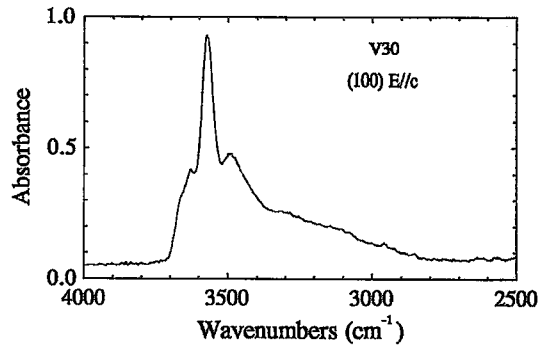

FIG. 7. The E ∥ *c* absorption-spectra of V30 in the principal hydroxyl-stretching frequency region, with an expanded range either side of the major absorptions. Note the broad low-amplitude absorption that extends down to ~2800 cm^{-1}.

~2500 cm^{-1}; this is shown in an expanded range for the E ∥ *c* spectrum of V30 in Figure 7. This absorption is a real feature and is present in many of the spectra.

The previous discussion gives a general framework within which we can now attempt a detailed assignment of all bands in all spectra, taking into account the variation in chemical composition of the crystals examined. Initially, we will consider the spectra of boron-free vesuvianite.

Boron-Free Vesuvianite

Although the spectra in this group show broad similarities, there are significant variations that correlate with changes in composition, specifically the extent of the $F^- \rightleftharpoons (OH)^-$ substitution and the nature of the cation substitutions at those sites that directly coordinate the *OH* and *O*(10) sites.

Fluorine-free vesuvianite

The spectra of V13 are shown in Figure 8. The (100) spectrum (Fig. 8a) shows very strong polarization, with maximum absorbance where E ∥ *c*. The spectrum is very unusual, with its continuous absorption between 3500 and 3000 cm^{-1}, and the very broad bands. There are (at least) nine discernable bands (Table 3), and there is also the suggestion of fine structure in some of the bands. The spectra for V11 and V23 are similar, showing only minor differences in resolution and band intensities that can be related to minor differences in composition. These compositions show a prominent *I* band whose polarization is incompatible with current ideas on the configurations of hydrogen-bonding in vesuvianite. This band is also of very unusual shape. It is centered at ~3240 cm^{-1}, but its low-energy tail extends down to ~2800 cm^{-1} (Fig. 7). Figure 8a suggests that this band is fairly symmetrical; if this is the case, a considerable amount of the absorption intensity in the higher-energy range (above 3400 cm^{-1}) will be due to the high-energy tail of this band. This will significantly affect our estimate of the intensities of the bands in this region, and requires further consideration; this will be done later.

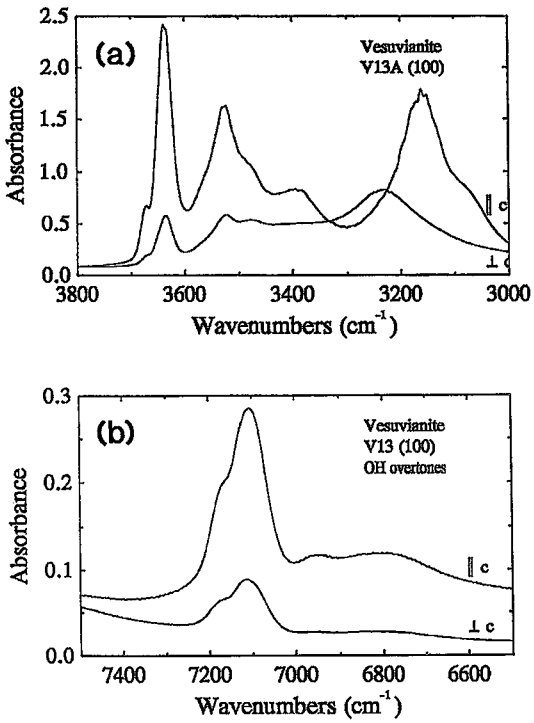

FIG. 8. The polarized absorption-spectra of fluorine-free vesuvianite V13 (a) in the principal hydroxyl-stretching region, and (b) in the hydroxyl-stretching overtone region.

The corresponding overtone spectra for V13 (Fig. 8b) are significantly less complex than the spectra in the fundamental region, but still show considerable detail. Again, the polarization dependence is E ∥ *c* > E ⊥ *c* for all bands. The principal features are a partly resolved doublet at ~7130 and ~7170 cm^{-1}, with much weaker and broader bands at ~6800 and ~6960 cm^{-1}. The spectra of V11 are similar, except that there is a single broad band at ~6850 cm^{-1} rather than the two absorptions seen in V13.

Fluorine-bearing vesuvianite

Spectra for V4 (3.5 F apfu) are shown in Figure 9. There are six principal absorptions and a broad sloping shoulder at ~3400 cm^{-1} in the E ∥ *c* spectrum of the principal hydroxyl-stretching region. As with fluorine-free vesuvianite, the absorption in both polarizations has a significant low-energy tail that extends down to ~2500 cm^{-1}. The enigmatic *I* band is present also in the E ⊥ *c* polarization, but is much weaker than in fluorine-free vesuvianite (*e.g.*, Fig. 8a).

The corresponding overtone spectra for V4 are shown in Figure 9b; spectra for V5 and V49 are very similar except for slight differences in resolution. The principal feature is a partly resolved doublet at ~6960 and ~7010 cm^{-1}, with a much weaker single band at ~6740 cm^{-1}; polarization dependence is E ∥ *c* > E ⊥ *c*.

Samples V6, V28 and V31 contain intermediate amounts of F (~2.0 apfu); by and large, the spectra (Fig. 10) are intermediate between the spectra of fluorine-free vesuvianite (Fig. 8) and those of fluorine-rich vesuvianite (Fig. 9). The spectra of V28 (Fig. 10) show considerable differences from the spectra of V4 (Fig. 9); positions and polarization dependencies of the major bands are the same, but the band intensities are radically different. In addition, the E ⊥ *c* spectrum shows less fine-structure in V28.

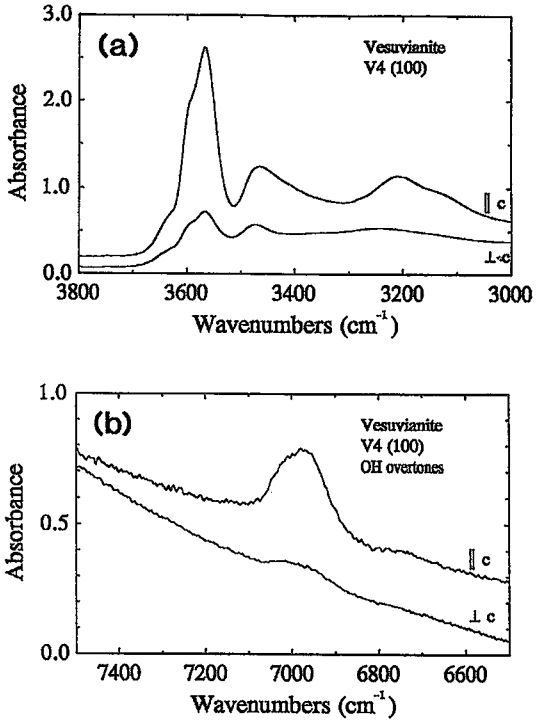

FIG. 9. The polarized absorption-spectra of fluorine-rich vesuvianite V4 (a) in the principal hydroxyl-stretching region, and (b) in the hydroxyl-stretching overtone region.

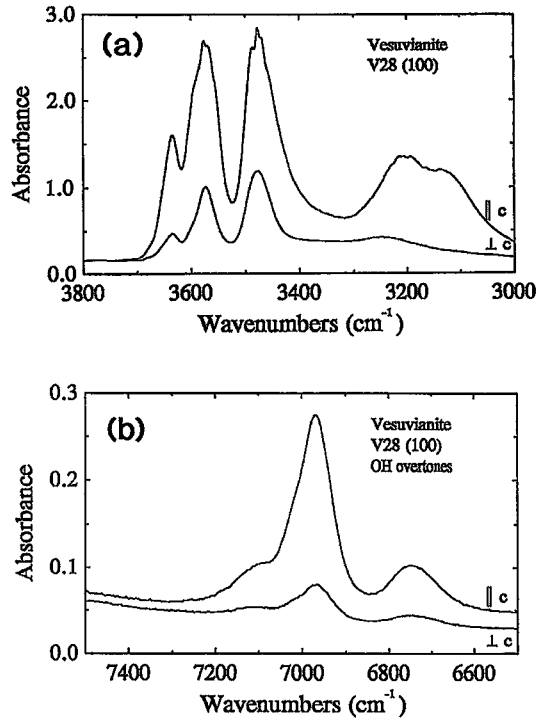

FIG. 10. The polarized absorption-spectra of fluorine-bearing vesuvianite V28 (a) in the principal hydroxyl-stretching region, and (b) in the hydroxyl-stretching overtone region.

The overtone spectra for V28 differ somewhat from those of V4. Instead of an obvious doublet, there is a strong single band at ~6970 cm^{-1}, with a slight suggestion of a shoulder at ~7010 cm^{-1}. There is a low-energy band at ~6750 cm^{-1} that is very symmetrical. The other significant difference from V4 is the prominent shoulder at ~7120 cm^{-1} in V28; comparison with V4 does show a slight asymmetry in the tail of the strong doublet, which could correspond to a very weak analogue of the prominent shoulder in V28.

BORON-BEARING VESUVIANITE

The spectra of V75 (2.4 apfu B) are shown in Figure 11. There is an extremely strong absorption at ~3580 cm^{-1}, with subsidiary maxima at ~3630 and ~3480 cm^{-1}, and these have very strong polarization, with maximum absorption for E ∥ *c*. At lower energies, there is a broad absorption at ~3150 cm^{-1} that is present in the E ∥ *c* spectrum and is completely absent in the E ⊥ *c* spectrum. In addition, there is the suggestion of some fine-structure in the high-energy band at ~3680 cm^{-1}.

The overtone spectra (Fig. 11b) show intensities E ∥ *c* > E ⊥ *c*. The strongest band occurs at ~6960 cm^{-1}, and there is a broad doublet to higher energies with component bands at ~7160 and ~7100 cm^{-1}, respectively. In addition, there is a broad weak band at ~6770 cm^{-1}. The spectra of V38 are similar, except that the doublet character of the high-energy absorption is not apparent.

Comparison of the spectra of samples with different boron contents (Fig. 12) shows the dramatic spectral differences produced by the incorporation of boron into the structure. Both the *OH* (bands *A–H*) and the *O*(10) (bands *J–M*) regions are affected, indicating that the direct substitution of boron for hydrogen, B + Mg ⇌ 2H + Al, proposed by Groat *et al.* (1992a) affects both hydrogen positions. Detailed structural work (Groat *et al.* 1994a) shows that boron replaces hydrogen at the *OH* position (Fig. 13). This obviously destroys configurations 1–4 (Table 5) and gives rise to new configurations specifically resulting in bands *D* and *F*; these are also present in crystals of the boron-free fluorine-rich vesuvianite, indicating that although these bands are at approximately the same energy, they arise from different local atomic configurations in the structure.

There is another key difference between the spectra of boron-bearing and boron-free vesuvianite. For E ⊥ *c*

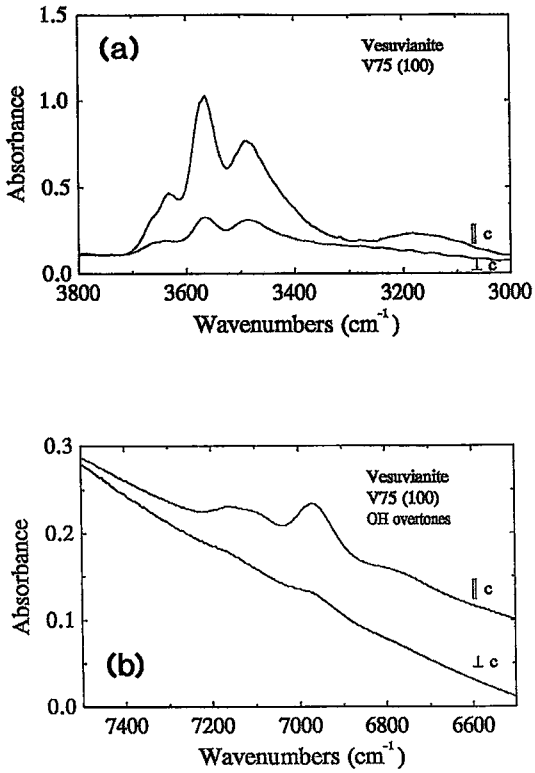

FIG. 11. The polarized absorption-spectra of boron-bearing vesuvianite V75 (a) in the principal hydroxyl-stretching region, and (b) in the hydroxyl-stretching overtone region.

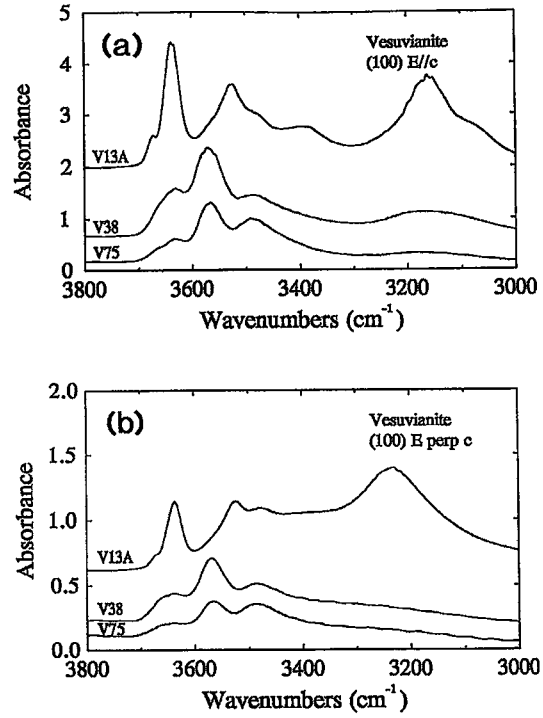

FIG. 12. Comparison of the spectra of vesuvianite crystals V13A, V38 and V75 in the principal hydroxyl-stretching region, showing the effect of different amounts of boron on the appearance of the spectra: (a) E ∥ *c* spectra; (b) E ⊥ *c* spectrum.

(Fig. 12b), the spectra of boron-free fluorine-free vesuvianite show a prominent *I* band that is absent in the spectra of boron-bearing vesuvianite; this observation strongly suggests that this band is due to the presence of hydrogen.

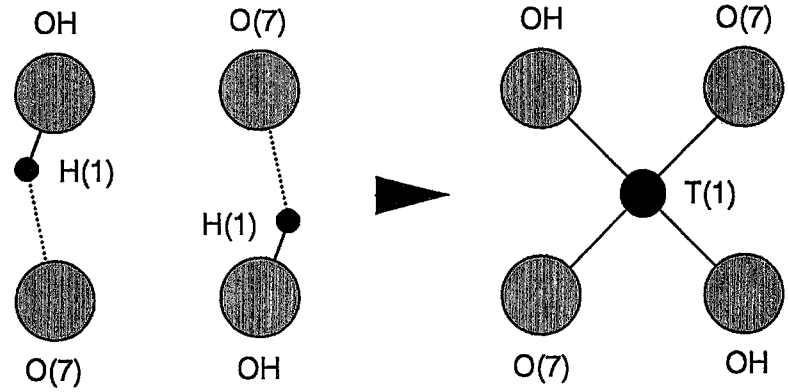

FIG. 13. The B + Mg → 2H + Al substitution in the vicinity of the *OH* sites (from Groat *et al.* 1994a).

Band Intensities in the Principal OH-Stretching Region

There have been many attempts to correlate band intensities in the principal OH-stretching region with cation occupancies at the sites coordinating the $(OH)^-$ anion [see Hawthorne (1981) and Rossman (1988) for reviews]. By and large, these attempts have not been very successful. There are several reasons for this, one of the more important being the fact that the molar absorptivity of an absorption band in this region is strongly related to the frequency (energy) of the band. Skogby & Rossman (1991) have shown that the molar absorptivity of OH bands in amphiboles can vary by a factor of 3 over a frequency range of ~ 100 cm^{-1}. If this type of behavior is generally the case, it accounts for several of the unusual features observed in the spectra of vesuvianite.

The range of significant absorption in vesuvianite is from ~ 3700–3000 cm^{-1} (perhaps in some cases down to 2500 cm^{-1}), a range of 700–1200 cm^{-1}. The vesuvianite spectra suggest that the molar absorptivity varies significantly over the observed spectral range. Samples V11 and V13 each have $8(OH)^-$ at the *OH* position and $1(OH)^-$ at the *O*(10) position; if the molar absorptivity of $(OH)^-$ were independent of frequency, then the relative intensities of the *OH* bands (*A–H*) should be eight times the intensity of the *O*(10) bands (*J–M*). Examination of Figures 6 and 8 shows that the relative intensities of the two groups of bands are more like 2:1 or 3:2 than 8:1 (omitting the *I* band from consideration). This suggests that the molar absorptivity increases significantly with decreasing band-frequency [albeit less so than that suggested by linear extrapolation of the curve for amphiboles published by Skogby & Rossman (1991)].

Band Width as a Function of Frequency

At the high-frequency end of the principal OH-stretching region, the *A* band is quite sharp (half-width ≈ 20 cm^{-1}), whereas at the low-frequency end, the bands are very broad (half-width ≈ 100 cm^{-1}). The half-width (full width at half height) of each band was measured with a mm scale for those spectra in which the band could be adequately resolved by eye. Although a relatively crude procedure, a systematic behavior of half width as a function of frequency (Fig. 14) is apparent; a very well-developed nonlinear correlation is present, the two lines in Figure 14 being drawn to emphasize this effect.

There are two significant features conveyed by Figure 14: (1) the increased band-broadening with decreasing frequency, and (2) the nonlinear aspect of this behavior. Feature (1) is due to increasing interaction with other structural vibrations as the strength of the hydrogen bond increases. Feature (2) does not seem to have been noted before, but does correlate with the two different environments of H in the vesuvianite structure. Bands *A–H* are associated with the *OH–H*(1)

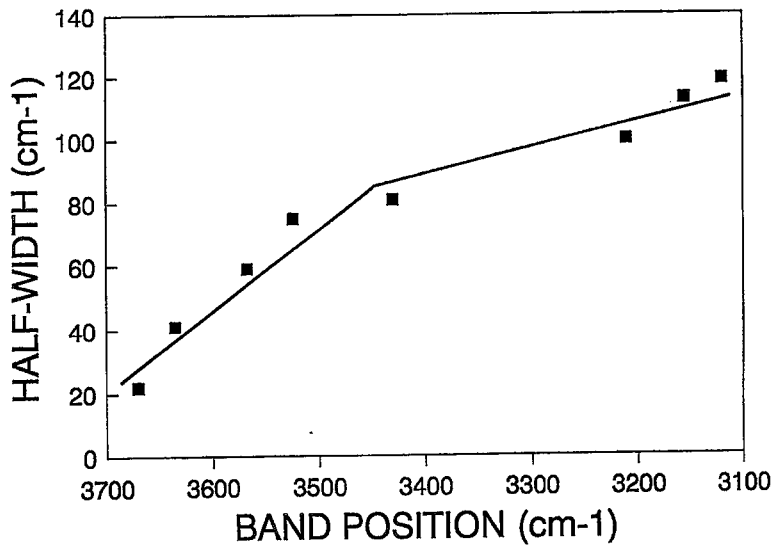

FIG. 14. Band half-width as a function of band frequency in the principal OH-stretching region for vesuvianite polarized E ∥ *c*; the line is drawn merely as a guide to the eye.

bond, and constitute the first (steeper) part of the curve in Figure 14. Bands *J–M* are associated with the *O*(10)–*H*(2) bond, and form the second (shallower) part of the curve. The *OH–H*(1) bond forms a bent hydrogen-bond system [*OH–H*(1)...*O*(7) ≈ 160°; Lager *et al.* 1989], whereas the *O*(10)–*H*(2) bond is part of a straight hydrogen-bond system [*O*(10)–*H*(2)...*O*(10) = 180°]. It is tempting to ascribe the different trends in Figure 14 to this feature, particularly as careful studies of hydrogen-bond geometry (Brown 1976) suggest that bent hydrogen-bonds and straight hydrogen-bonds are energetically distinct. If this is actually the case, the behavior shown in Figure 14 should be characteristic of OH-bearing crystals in general; this is currently under examination.

Detailed Assignment of Bands: The OH Site

The relative intensities of the *A–H* bands will now be related to the occupancies of the *Y*(3) site (as well as the F content), bearing in mind the effect of frequency on band intensity discussed above; site populations for the *Y*(3) site are shown in Table 6 for the crystals used in this work.

Boron-free vesuvianite

Inspection of Table 6 indicates that the dominant local *Y*(3)–*Y*(2) configuration must be configuration 1 of Table 5. In particular, samples V11, V13 and V23 are poor in fluorine and will not be affected by fluorine-blocking or additional fluorine-shifted bands; hence their spectra must consist predominantly of bands due to configurations 1–4 in Table 5. In V11 and V13, the strongest E ∥ *c* band is *B* at ~3630 cm^{-1}; this must be due to configuration 3 (Table 5). By analogy with other hydroxyl-bearing minerals (amphiboles, micas, talc; Hawthorne 1981, Rossman 1988), bands due to configurations involving lighter lower-valent species will occur at higher frequencies; thus the *A* band will be due to configuration 1 (Table 5).

The most intense bands in V49 are *B*, *D* and *F* (Fig. 3), the only *Y*(3) cations are Al and Mg (Table 6), and there is 4.1 F apfu. Thus the possible configurations in V49 are 1, 3, 5 and 7 (Table 5). We have already assigned band *A* to configuration 1, and band *A* is absent in the V49 spectrum (Fig. 3). Hence F must preferentially order at *OH* sites coordinated to Mg and Al, producing configuration 5 rather than configuration 1. Band *B* is already assigned to configuration 3, and thus bands *D* and *F* must correspond to configurations 5 and 7; note that this in reasonable accord with the occupancy of the *Y*(3) site in V49. Which of the bands *D* and *F* is due to which of the two possible configurations, 5 and 7, cannot be determined on the compositions of the *Y*(3) site only, as the relative intensities of the bands also depend on the local order exhibited by F^- (*cf.* Figs. 5b, c). However, a higher-charge substituent cation usually displaces the principal hydroxyl-stretching band to lower frequencies than lower-charge substituents; on the strength of this argument, we provisionally assign bands *D* and *F* to configurations 5 and 7, respectively.

We have ascribed the *A*, *B*, *D*, and *F* bands to configurations involving Mg or Al at *Y*(3); the *C*, *E*, *G*, *H* bands must therefore be due to configurations involving Fe^{2+} or Fe^{3+} at *Y*(3). The relative weakness of these bands in the spectra (Figs. 3a, b) is in accord with the general low level of Fe^{2+} and Fe^{3+} at the *Y*(3) sites in these crystals (Table 6).

TABLE 6. APPROXIMATE *Y*(3)-SITE, F AND B CONTENTS (APFU) IN THE VESUVIANITE CRYSTALS STUDIED

	Al	Mg	Fe^{2+}	Fe^{3+}	F	B
V4	5.2	1.2	0.5	1.1	3.1	–
V5	5.7	1.3	0.6	0.4	3.5	–
V6					3.9	–
V11	6.7	1.3	–	–	–	–
V13	6.3	1.2	–	0.5	–	–
V23	6.3	1.7	–	–	–	–
V28	5.4	1.3	1.1		2.0	–
V30	2.8	3.8	1.4		1.2	2.6
V31	5.6	1.1	1.1		2.4	–
V33	5.9	1.3	0.8	0.1	4.8	–
V38	2.9	3.5	1.6		1.2	1.5
V45	4.1	2.9	1.0		1.0	1.2
V49	6.8	1.2	–		4.1	–
V75	2.9	4.6	–	0.4	0.4	2.4

Boron-bearing vesuvianite

The incorporation of boron at the *T*(1) site (Fig. 13) will have a direct effect on the hydroxyl-stretching spectra as B replaces two hydrogen atoms and reduces the overall intensity of absorption (Fig. 12). However, its incorporation can also potentially have an inductive effect. Removal of one hydrogen atom in a trimer and replacement of the H–O bond by a B–O bond may inductively change the strength of the O–H bond in the *trans OH* of the trimer (Fig. 13b), producing a new band in the hydroxyl-stretching region. As is apparent in Figure 12, incorporation of boron into the structure does correlate with a radical reduction in the intensity of the *A*, *B* and *E* bands, and the appearance or strong relative increase in intensity of the *D* and *F* bands. Above, we have ascribed these two bands to configurations 5 and 7, the Mg–Al–F and Al–Al–F configurations. The dominance of these two bands in the boron-bearing vesuvianite spectra indicates that the

inductive effect of boron substitution at the $T(1)$ site (Fig. 13b) is similar to the inductive effect of fluorine substitution at the *OH* site (Fig. 5c). This being the case, we expect band *D* to be more dominant than band *F* in the spectra of boron-bearing vesuvianite, as these have Mg greater than Al. However, note that the situation is slightly complicated by the fact that the crystals of boron-bearing vesuvianite also contain some fluorine, and hence will also have some component of the *D* and *F* bands due to the inductive effect of fluorine as well as that of boron.

Careful inspection of the *F* band in the spectra of boron-bearing vesuvianite (Figs. 3a, 12) shows it to occur at slightly different frequencies in the spectra of the boron-bearing (~3485 cm^{-1}) and fluorine-bearing boron-free vesuvianite (~3470 cm^{-1}), showing that the dominant configuration giving rise to this band is different in each compositional variant.

TABLE 8. APPROXIMATE *Y*(1)-SITE CONTENT* (APFU) IN THE VESUVIANITE CRYSTALS STUDIED

	Ti	Fe^{2+}	Fe^{3+}	Mg	Al
V4	0.5	0.5	–	–	–
V5	0.4	0.6	–	–	–
V6	0.4	0.6		–	–
V11	–	0.5			0.5
V13	0.2	0.6	0.2	–	–
V23	–	0.2	0.4		0.2
V28	1.0	–		–	–
V30	0.2	0.8		–	–
V31	1.0	–		–	–
V33	0.2	0.8	–	–	–
V38	0.5	0.5		–	–
V45	0.5	0.5		–	–
V49	–	0.5			0.2
V75	0.1	0.7	0.2	–	–

Detailed Assignment of Bands: The *O*(10) Site

Boron-free vesuvianite

Inspection of Table 7 and Figure 3 shows that the boron-free crystals fall into two groups; V11 and V13, and the rest (V4, V5, V6, V28, V31, V49). Both V11 (Fig. 6) and V13 (Fig. 8) show strong *K* and *M* bands. Both V11 and V13 are hydroxyl-rich and (nearly) fluorine-free; the *Y*(1) site populations (Table 8) are approximately [0.4Fe^{2+} + 0.5(Mg + Al)] and [0.2Ti + 0.6Fe^{2+} + 0.2(Mg + Al)], respectively. The local hydrogen-bonding configuration must be dominated by O–O occupancy of adjacent *O*(10) sites (Fig. 15a). Thus the *K* and *M* bands must represent occupancy of *Y*(1) [bonded to $(OH)^-$] by two different cations. Inspection of Table 8 shows that in V13, *Y*(1) is dominated by Fe^{2+}, whereas in V11, *Y*(1) contains similar amounts of Fe^{2+} and (Mg,Al). Thus band *K* seems associated with Fe^{2+} occupancy of *Y*(1), whereas band *M* is associated with (Mg, Al, Fe^{3+}?) occupancy of *Y*(1).

The other crystals (V4, V5, *etc.*) all contain significant amounts of fluorine. Groat *et al.* (1992b) have shown that fluorine preferentially occupies the *O*(10) site, up to 1 apfu; in this case, the dominant hydrogen-bonding configuration corresponds to $(OH)^-$–F^- occupancy of adjacent *O*(10) sites (Fig. 15b). The *J* and *L* bands also must represent occupancy of *Y*(1) by two different cations. Inspection of Table 8 shows these cations to be Fe^{2+} and Ti^{4+}. As V5 has Fe^{2+} greater than Ti^{4+} and *J* greater than *L*, this suggests that band *J* is associated with Fe^{2+} at *Y*(1), and band *L* is associated with Ti^{4+} at *Y*(1).

TABLE 7. INTENSITIES* FOR BANDS J–M IN THE VESUVIANITE CRYSTALS STUDIED

	J	*K*	*L*	*M*
V4	10	**–	2	–
V5	20	–	4	–
V6	20	–	10	–
V11	2	30	–	25
V13	–	35	–	5
V28	20	–	15	–
V30	–	–	–	–
V31	15	–	10	–
V38	5	———	5	–
V45	5	———	5	–
V49	10	–	8	–
V75	2	———	2	–
ALA				
GEM		?		–

* values estimated by eye from Figure 3.
** – denotes band not observed.

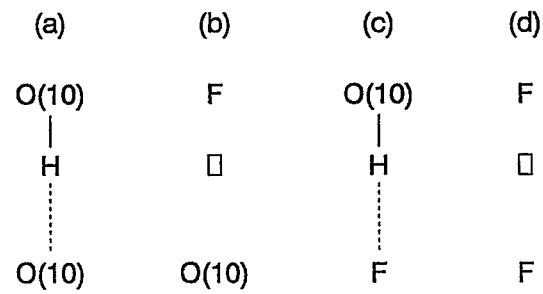

FIG. 15. Possible OH–F arrangements at adjacent *O*(10) sites: (a) OH^-–OH^-; (b) OH^-–F; (c) F–F; after Groat *et al.* (1992b).

Boron-bearing vesuvianite

As noted above, boron directly replaces hydrogen at the *H*(2) site, leading to significant reduction or even complete loss of intensity in the low-frequency region (bands *I–M*) of the spectrum. It is also notable that only one broad band is present in this region in crystals V38, V45 and V75. In V45 and V75, this band is symmetrical, but in V38 (Fig. 12), this band shows a slight asymmetry, suggesting that it consists of two components; presumably this is also the case for V45 and V75. Thus the *J* and *L* bands are the predominant bands of this region in the spectra of boron-bearing vesuvianite, and it is notable that all these crystals do contain significant amounts of fluorine (Table 2).

Overtone Spectra

Band positions are given in Table 4. Also shown in Table 4 are the corresponding fundamental bands and the ratio $\upsilon^{\circ}/2\upsilon^{F}$, where υ° and υ^{F} are the frequencies of the overtone and fundamental bands, respectively; the latter values are a measure of the degree of anharmonicity involved in the O–H interaction. The polarization behavior also corresponds with that observed in the fundamental region. Although the overtone spectra lack the fine detail of the fundamental spectra, they are equally diagnostic of the behavior of the O–H bonds in vesuvianite, and do not require the sample to be thinned to the same extent in order to record the spectra.

Comparison of Figure 3 and Table 3 with Figure 4 and Table 4 shows that, whereas bands *A–F* in the fundamental region have readily apparent counterparts *A′–F′* in the (first) overtone region, the corresponding overtone of the lower-frequency fundamental bands (especially *J* and *K*) are apparent only after careful inspection. In the fundamental region, V30 has no *J* or *K* bands, whereas GEM has a very strong *K* band (Fig. 3). Comparison of the overtone spectra (Fig. 16) shows that GEM has a weak band at ~5930 cm^{-1} in the E ∥ *c* polarization, whereas V30 has no such band. If this band is the *K′* overtone, it should also be present in other crystals with strong *K* bands. As shown in Figure 17, this is the case. Crystal V13 has a strong *K* band in the fundamental region (Fig. 3) and also has a discernable *K′* band at ~5930 cm^{-1}; crystals V5 and V30 show no *K* band and weak *J* and *L* bands, and have no relatively strong band in the 5500–6500 cm^{-1}

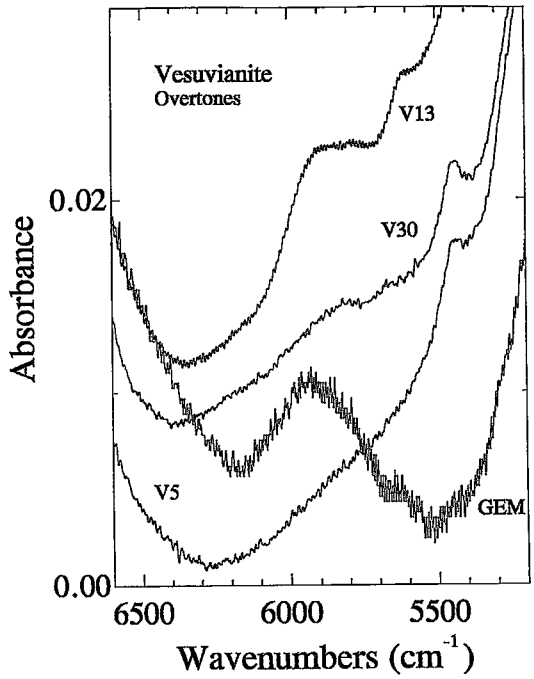

FIG. 17. The E ∥ *c* overtone spectra of vesuvianite crystals with (V13, GEM) and without (V5, V30) significant overtone bands at 5930 cm^{-1}.

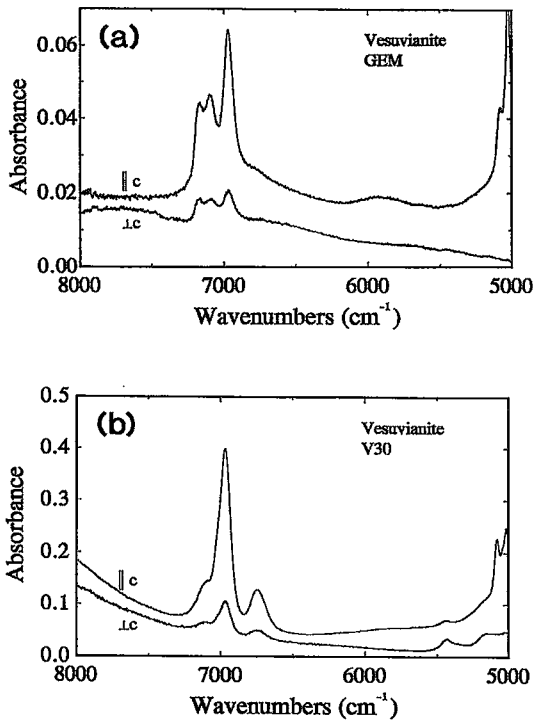

FIG. 16. The polarized absorption spectra of vesuvianite in the hydroxyl-stretching overtone region: (a) GEM, which shows a weak band polarized E ∥ *c* at ~5930 cm^{-1}; (b) V30, which shows no band near 5900 cm^{-1}.

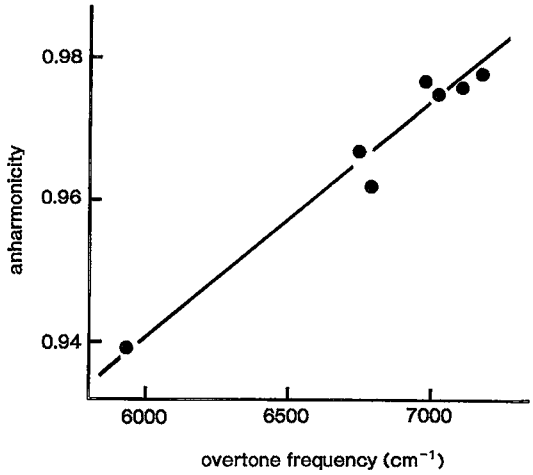

FIG. 18. Variation in anharmonicity ($\upsilon^{\circ}/2\upsilon^{F}$) as a function of the frequency of the first hydroxyl-stretching overtone band in vesuvianite.

region; the position and anharmonicity factor of this *K'* band are listed in Table 4. As shown in Figure 18, the anharmonicity ratio correlates fairly well with the frequency of the overtone band, further supporting the assignment of *K'* as first overtone of OH.

The O–H interaction is quite anharmonic, the longer O–H bonds correlating with increasing anharmonicity. Longer O–H bonds also correlate with decreasing principal-stretching frequency. Consequently, as the principal-stretching frequency decreases, the anharmonicity should increase; this is exactly what is observed (Fig. 18). The band width increases as a function of frequency for the overtone spectra, in line with what is observed (Fig. 14) for the fundamental bands.

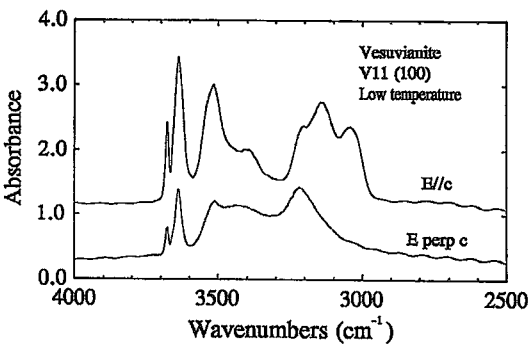

FIG. 19. Spectra of vesuvianite V11 taken at the temperature of liquid N_2; the low-frequency undulations in the baseline away from the OH features are interference fringes.

LOW-TEMPERATURE SPECTRA

In an effort to increase the resolution of the spectra, a few samples were run at the temperature of liquid N_2. Figure 19 shows the polarized low-temperature spectra for V11 in the principal OH-stretching region. Comparison with the room-temperature spectra (Fig. 6) shows that although the bands sharpen somewhat at low temperature, no additional bands are observed as a result of this slightly increased resolution; however, note that the very broad absorption at ~3230 cm^{-1} in the $E \perp c$ polarization still extends down to well below 3000 cm^{-1}.

SUMMARY

There is considerable variation in the principal OH-stretching spectra of vesuvianite, more so than any other mineral species in which hydrogen is a major element; the principal spectral features are listed below.

1. There are 13 recognizable bands (*A–M*) that may be divided into three types: (i) Eight bands (*A–H*) are polarized, with intensities $E \parallel c \approx 8$, $E \perp c \approx 2$; these are due to principal OH-stretching absorptions at the *OH* site. (ii) One band (*I*) is polarized with $E \perp c \approx 10$; this behavior is not compatible with the assignment of this band to a simple OH-stretching vibration in the structure; the origin of this band will be discussed elsewhere. (iii) Four bands (*J–M*) are polarized with $E \parallel c = 10$; these are due to absorption at the *O*(10) site.
2. The eight bands *A–H* are due to different local configurations of cations at *Y*(3) site, which bonds to *OH*, and to different local configurations of anions [OH^-–OH^- and OH^-–F^-] at adjacent *OH* sites.
3. The four bands J–*M* are due to different local configurations of cations at *Y*(1), and to different local configurations of anions [OH^-...O^{2-} and OH^-...F^-] at adjacent *O*(10) sites.
4. Implicit in points 2 and 3 is the great effect that the incorporation of fluorine has on the principal OH-stretching spectra. Vesuvianite exhibits classical two-mode behavior in this respect, but the resultant bands are degenerate with bands in fluorine-free vesuvianite.
5. Boron is incorporated into the vesuvianite structure primarily *via* the substitution $B + Mg \rightleftharpoons 2H + Al$, and hence has a drastic effect on the OH-stretching spectra. In boron-rich crystals, the four bands *J–M* are not present, indicating that hydrogen has been completely replaced in the vicinity of the *O*(10) site. The absolute intensity of the spectra is also greatly decreased by this substitution, and the relative intensities of the bands *A–H* are also strongly affected.
6. Although lacking the fine detail of the OH-stretching spectra in the principal-stretching region, the overtone spectra show equally diagnostic spectral

behavior.

7. The spectra in the principal OH-stretching region extend over a very wide range (3600–3000 cm^{-1}, or even lower), and show two very important features that are of general importance in interpreting such spectra: (i) the band width increases significantly with decreasing band-frequency, and (ii) the band intensity is nonlinearly correlated with band frequency.

Acknowledgements

We are grateful to the Department of Mineralogy, Royal Ontario Museum, for many of the samples used in this work. Financial support was provided by the Natural Sciences and Engineering Research Council of Canada in the form of operating grants to LAG and FCH, and by the White Rose Foundation and the National Science Foundation grant EAR89–16064 to GRR. We thank the reviewers and Associate Editor Georges Calas for their helpful comments.

References

Brown, I.D. (1976): On the geometry of O–H...O hydrogen bonds. *Acta Crystallogr.* **A32**, 24-31.

Coda, A., Della Giusta, A. Isetti, G. & Mazzi, F. (1970): On the crystal structure of vesuvianite. *Atti Accad. Sci. Torino* **105**, 63-84.

Eby, R.K., Janeczek, J., Ewing, R.C., Ercit, T.S., Groat, L.A., Chakoumakos, B.C., Hawthorne, F.C. & Rossman, G.R. (1993): Metamict and chemically altered vesuvianite. *Can. Mineral.* **31**, 357-369.

Fitzgerald, S., Leavens, P.B., Rheingold, A.L. & Nelen, J.A. (1987): Crystal structure of a REE-bearing vesuvianite from San Benito County, California. *Am. Mineral.* **72**, 625-628.

_____, Rheingold, A.L. & Leavens, P.B. (1986a): Crystal structure of a Cu-bearing vesuvianite. *Am. Mineral.* **71**, 1011-1014.

_____, _____ & _____ (1986b): Crystal structure of a non-*P4/nnc* vesuvianite from Asbestos, Quebec. *Am. Mineral.* **71**, 1483-1488.

Giuseppetti, G. & Mazzi, F. (1983): The crystal structures of a vesuvianite with *P4/n* symmetry. *Tschermaks Mineral. Petrogr. Mitt.* **31**, 277-288.

Groat, L.A., Hawthorne, F.C. & Ercit, T.S. (1992a): The chemistry of vesuvianite. *Can. Mineral.* **30**, 19-48.

_____, _____ & _____ (1992b): The role of fluorine in vesuvianite: a crystal-structure study. *Can. Mineral.* **30**, 1065-1075.

_____, _____ & _____ (1994a): The incorporation of boron into the vesuvianite structure. *Can. Mineral.* **32**, 505-523.

_____, _____ & _____ (1994b): Excess *Y*-group cations in the crystal structure of vesuvianite. *Can. Mineral.* **32**, 497-504.

_____, _____, _____ & Putnis, A. (1993): The symmetry of vesuvianite. *Can. Mineral.* **31**, 617-635.

Hawthorne, F.C. (1981): Amphibole spectroscopy. *In* Amphiboles and Other Hydrous Pyriboles – Mineralogy (D.R. Veblen, ed.). *Rev. Mineral.* **9A**, 103-139.

Howard, S.A. & Preston, K.D. (1989): Profile fitting of powder diffraction patterns. *Rev. Mineral.* **20**, 217-275.

Lager, G.A., Xie, Q., Ross, F.K., Rossman, G.R., Armbruster, T., Rotella, F.J. & Schultz, A.J. (1989): Crystal structure of a *P4/nnc* vesuvianite from Tanzania, Africa. *Geol. Soc. Am., Abstr. Programs* **21**, A120.

Rossman, G.R. (1988): Vibrational spectroscopy of hydrous components. *In* Spectroscopic Methods in Mineralogy and Geology (F.C. Hawthorne, ed.). *Rev. Mineral.* **18**, 193-206.

Rucklidge, J.C., Kocman, V., Whitlow, S.H. & Gabe, E.J. (1975): The crystal structures of three Canadian vesuvianites. *Can. Mineral.* **13**, 15-21.

Skogby, H. & Rossman, G.R. (1991): The intensity of amphibole OH bands in the infrared absorption spectrum. *Phys. Chem. Minerals* **18**, 64-68.

Valley, J.W., Peacor, D.R., Bowman, J.R., Essene, E.J. & Allard, M.J. (1985): Crystal chemistry of a Mg-vesuvianite and implications of phase equilibria in the system $CaO–MgO–Al_2O_3–SiO_2–H_2O–CO_2$. *J. Metamorph. Geol.* **3**, 137-153.

Warren, B.E. & Modell, D.I. (1931): The structure of vesuvianite $Ca_{10}Al_4(Mg,Fe)_2Si_9O_{34}(OH)_4$. *Z. Kristallogr.* **78**, 422-432.

Yoshiasa, A. & Matsumoto, T. (1986): The crystal structure of vesuvianite from Nakatatsu mine: reinvestigation of the cation site-population and of the hydroxyl groups. *Mineral. J.* **13**, 1-12.

Received July 16, 1993, revised manuscript accepted October 6, 1994.